Improved Karplus Equations for $^3J_{C1,H4}$ in Aldopentofuranosides: Application to the Conformational Preferences of the Methyl Aldopentofuranosides

Justin B. Houseknecht,* Todd L. Lowary,* and Christopher M. Hadad*

Department of Chemistry, The Ohio State University, Columbus, Ohio 43210

Received: July 25, 2002; In Final Form: October 30, 2002

The effects of electronegativity and stereochemistry upon three bond ^{1}H−^{1}H coupling constants ($^3J_{H,H}$) are widely appreciated and have been taken into consideration in the development of Karplus equations for H−C−C−H fragments. These equations have found particular use in the conformational analysis of molecules containing aldopentofuranose residues. This paper demonstrates the effect of anomeric stereochemistry upon $^3J_{C1,H4}$ in aldopentofuranosides and proposes Karplus equations that account for this effect. These new equations are shown to provide improved results for the determination of furanose ring conformation when compared to those obtained solely with $^3J_{H,H}$ data. The equations described here should be applicable to furanose derivatives containing any substituent at the anomeric center.

Introduction

It is difficult to overstate the importance of the furanose ring in biology. These moieties are found as constituents of nucleic acids,[1] bacterial, parasitic, and fungal cell wall polysaccharides,[2] as well as other natural products.[3] A key characteristic of these ring systems is their inherent flexibility, which profoundly influences their role in biological processes. Consequently, understanding the conformational preferences of furanose rings is an important area of research.

Given their presence in nucleic acids, early studies in the area of furanose conformation focused on defining the conformational preferences of the sugar residues present in DNA and RNA, 2-deoxy-β-D-*erythro*-pentofuranose and β-D-ribofuranose, respectively.[1] The analysis of a large number of nucleoside crystallographic structures by Altona and Sundaralingam led to the development of a model that can be used to describe the conformational preferences of any furanose ring.[4,5] This model makes use of the pseudorotational wheel (Figure 1) to describe the possible ring conformers. Structurally similar conformers are located near one another on the wheel such that only small conformational distortions between twist (T) and envelope (E) conformers are required for pseudorotation[6] between adjacent conformers. Although there are 20 idealized E and T conformations, furanose rings can adopt an infinite number of conformations that differ slightly from these ideal geometries. Each conformer can be described by two parameters, the pseudorotational phase angle (P) and the puckering amplitude (Φ_m), which can be calculated from five endocyclic torsion angles of the ring.[4,5] The relationship between the P value and the various conformers of a furanose ring is shown in Figure 1. In the model developed by Altona and Sundaralingam, the solution conformation of a furanose ring can be described as an equilibrium mixture of two conformers, one in each of the northern and southern hemispheres, termed the N and S conformers, respectively.

A method commonly used for determining the N and S conformers populated by a furanose ring in solution involves the measurement of three bond hydrogen−hydrogen NMR coupling constants ($^3J_{H,H}$) and the interpretation of these data through the use of appropriate Karplus equations.[7,8] These equations relate $^3J_{H,H}$ with a dihedral angle that can, in turn, be correlated with P and Φ_m. This analysis is most conveniently done via the computer program PSEUROT,[9] which assumes that the previously mentioned two state N/S model is valid. The PSEUROT approach has proven useful for determining the conformational preferences of numerous five-membered rings.[10] It has long been appreciated, however, that for most systems there is more than one set of conformer pairs that can reproduce the observed $^3J_{H,H}$.[7,11] Empirical, not experimental, methods are typically used to determine which set of mathematically possible conformers are physically feasible. For example, certain solutions are ruled out given that the conformers predicted have unlikely orientations of ring substituents, e.g., the C-4 hydroxymethyl group is placed in a pseudoaxial orientation. In other cases, it can be useful to compare the results of these analyses with available crystal structure data. However, the complexity of the problem sometimes precludes the empirical approach; therefore, an experimental solution to this problem would be advantageous.

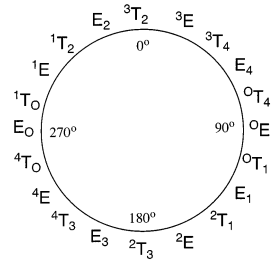

Figure 1. Pseudorotational itinerary for a D-aldofuranose ring.

Three bond ^{1}H−^{13}C coupling constants in furanose rings vary as a function of P, and it has been shown that these $J_{C,H}$ values are useful probes of ring conformation.[12] Of all of the $^3J_{C,H}$ present in a furanose ring, it appeared that $^3J_{C1,H4}$ would be the most straightforward to measure from proton-coupled ^{13}C NMR spectra of unlabeled substrates. The use of $^3J_{C1,H4}$ in the conformational analysis of furanose rings requires that a Karplus curve be available for relating the coupling constant magnitude to a dihedral angle. Although Karplus relationships for C−O−C−H fragments in carbohydrates have been reported,[13−15] the

* Address correspondence to Todd L. Lowary. E-mail: lowary.2@osu.edu.

10.1021/jp026610y CCC: $25.00
Published on Web 12/18/2002

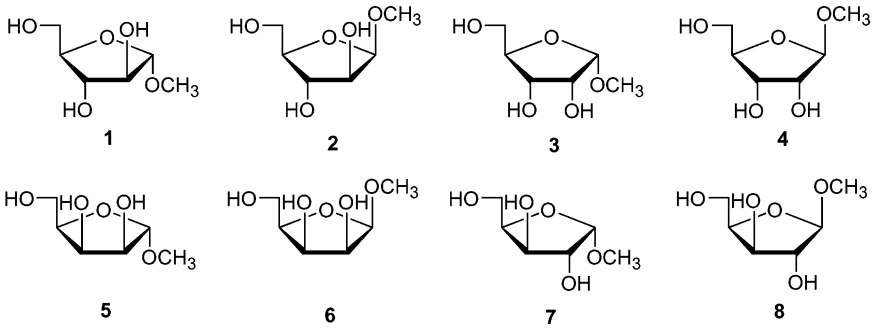

Figure 2. Methyl furanosides **1**−**8**. Methyl α-D-arabinofuranoside (**1**), methyl β-D-arabinofuranoside (**2**), methyl α-D-ribofuranoside (**3**), methyl β-D-ribofuranoside (**4**), methyl α-D-lyxofuranoside (**5**), methyl β-D-lyxofuranoside (**6**), methyl α-D-xylofuranoside (**7**), methyl β-D-xylofuranoside (**8**).

curves that have been derived by experimental means[13,14] vary markedly from one that was determined via computational methods.[15] In an effort to determine which curve to use, we calculated the $^3J_{C1,H4}$ values for some methyl furanosides (see below). These calculations showed that for the D-arabinofuranose ring system, the $^3J_{C1,H4}$ magnitudes for a given dihedral angle differed significantly as a function of anomeric stereochemistry, thus suggesting that the orientation of the aglycone is an important variable. However, none of the $^3J_{C,H}$ Karplus relationships reported to date have included terms to account for differences in the orientation of substituents along the coupling pathway. We have therefore developed an equation specific for $^3J_{C1,H4}$ in pentofuranosides parametrized such that the orientation and electronegativity of the C_1 substituent is taken into consideration. We have also measured $^3J_{C1,H4}$ in methyl pentofuranosides **1**−**8** (Figure 2) and have shown that the magnitude of this coupling constant can, in some cases, be used to clarify the results of PSEUROT calculations. The work reported here extends our earlier work focused on understanding the conformational preferences of furanosides and related molecules.[16]

Methods

Computational. Density functional theory (DFT)[17] calculations were performed using Gaussian 98[18] in the gas phase.[19] For each methyl furanoside **1**−**8**, 30 idealized envelope conformers were generated at the B3LYP/6-31G* level as previously reported.[20] The $^3J_{C1,H4}$ values were calculated for each B3LYP/6-31G*[21] optimized geometry using the deMon-KS program augmented by the deMon-NMR code.[22] The Perdew and Wang exchange and the Perdew correlation functional with the IGLO III[23] basis set were used for all of the deMon-NMR calculations. A FINE grid with 32 (for the calculation of the PSO and DSO contributions to spin−spin couplings) and 64 (for the FC term) points of radial quadrature was employed in the deMon-NMR calculations. These calculations provided a data set of 240 $^3J_{C1,H4}$ values, 120 with the α-stereochemistry at the anomeric center and 120 with the β-stereochemistry. In these conformers, all $C_1-O_4-C_4-H_4$ dihedral angles fall within a range between 80 and 150°. From a practical point of view, the lack of dihedral angles in the 0−80° and 150−180° range is not a concern as the constraints of the five-membered ring prohibit dihedral angles with these magnitudes. Therefore, although any Karplus curve resulting from a fit of these data may be poorly parametrized for $C_1-O_4-C_4-H_4$ dihedral angles around 0°, it will be well-parametrized for those dihedral angles that are normally present in five-membered rings.

Synthesis. All methyl furanosides were prepared from the respective reducing sugar by treatment with hydrochloric acid in methanol.[24] Anomers were purified by silica gel chromatography.

NMR Spectroscopy. NMR spectra were obtained on 300 mM solutions in D_2O at 27 °C at 500 (^{1}H) and 125 MHz (^{13}C). All ^{1}H NMR spectra matched those previously reported.[25] Additional ^{1}H NMR spectra were recorded at 35, 45, 55, 65, 75, and 85 °C. The $^3J_{C,H}$ values were measured from one-dimensional ^{13}C NMR spectra that were obtained by selective decoupling of coupled protons and first-order analysis.

PSEUROT Analysis. For all PSEUROT calculations using single temperature $^3J_{H,H}$ data, the Φ_m of both conformers was kept constant at 39° as computational and crystal structure data suggest that this is a reasonable puckering amplitude for these furanose ring systems.[20,26,27] In PSEUROT calculations using $^3J_{H,H}$ data measured from spectra recorded over a range of temperatures, the Φ_m of both conformers was allowed to optimize in addition to the *P* values and the relative populations. The values of the parameters *A* and *B* used were those previously calculated for these ring systems,[20] and the substituent electronegativities employed were as follows: 1.25 for OH, 1.26 for OR, 0.68 for CH_2OH, 0.50 for $CH(OR)_2$, and 0.0 for H. For each ring system, a series of four calculations (A−D) were carried out in which the starting *P* value of the N and S conformers were as follows: run A: $P_N = 50$, $P_S = 150$; run B: $P_N = 50$, $P_S = 250$; run C: $P_N = 320$, $P_S = 250$; and run D: $P_N = 320$, $P_S = 150$.

Results and Discussion

Previously Reported $^3J_{COCH}$ Karplus Equations. Three Karplus equations for $^3J_{COCH}$ in carbohydrates have previously been reported.[13−15] The Mulloy[13] and Tvaroska[14] equations were developed through the measurement of $^3J_{COCH}$ in rigid compounds for which crystal structures were available. By assuming that the C−O−C−H dihedral angles in these molecules were the same in solution as in the crystal structure, it was possible to derive $^3J_{COCH}$ Karplus equations. More recently, Serianni and co-workers used DFT calculations of disaccharide models to calculate $^3J_{COCH}$ values that were then used to develop a Karplus relationship.[15] In comparing the curves obtained from the experimental $^3J_{COCH}$ with the one developed from the computed coupling constants, discrepancies are evident, particularly for dihedral angles near 0 and 180° (Figure 3). To assess which equation would be best for the analysis of furanosidic glycosides, we calculated the $^3J_{C1,H4}$ in the envelope ring conformers of both methyl D-arabinofuranosides (**1** and **2**) using deMon-NMR. A comparison of these $^3J_{COCH}$ values (Figure 3) indicated that the anomeric stereochemistry does influence the magnitude of $^3J_{C1,H4}$ in these ring systems, with the β-glycoside coupl-

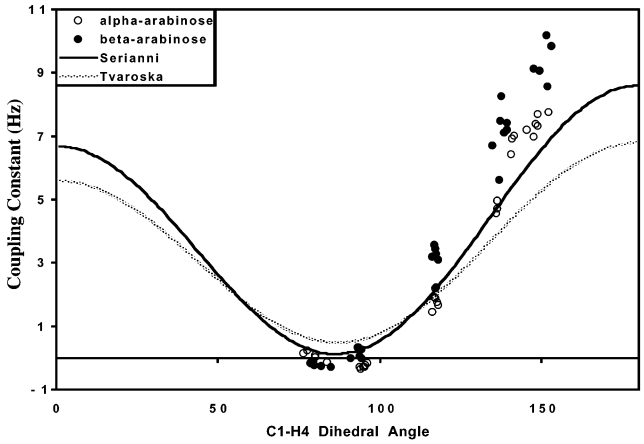

Figure 3. Comparison of Tvaroska (ref 14) and Serianni (ref 15) C−O−C−H Karplus curves with the deMon-NMR calculated $^3J_{C1,H4}$ values for **1** (open circles) and **2** (solid circles). The Mulloy (ref 13) and Tvaroska curves are essentially identical, and so only one of these curves is shown.

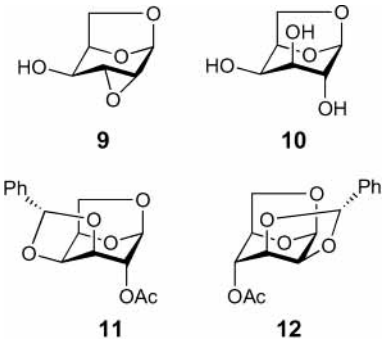

Figure 4. Compounds used to determine scaling factor for calculated $^3J_{C1,H4}$.

TABLE 1: Comparison of Calculated and Experimental $^3J_{COCH}$ for 9−12[a]

compound	path	exp $^3J_{C,O,C,H}$	calcd $^3J_{C,O,C,H}$	difference (%)
10[b]	C_1-H_{6endo}	1.4	1.90	19
	C_1-H_{6exo}	2.2	2.35	3
	C_1-H_5	5.6	6.18	15
11[b]	C_6-H_1	5.1	6.07	36
	C_5-H_1	5.1	5.26	7
	C_1-H_5	5.9	6.81	10
12[b]	C_7-H_4	2.3	2.88	25
	C_6-H_1	5.1	5.15	1
13[c]	C_7-H_2	2.8	3.81	36
	C_6-H_1	6.0	6.84	14
avg difference (%)				16.7

[a] Coupling constants are in Hz. [b] Ref 14. [c] Cano, F. H.; Foces-Foces, C.; Jimenez-Barbero, J.; Bernabe, M.; Martin-Lomas, M. *Carbohydr. Res.* **1986**, *155*, 1.

ings being, in general, larger than those of the α-glycosides for a given C_1-H_4 dihedral angle. This suggested that the previously reported $^3J_{COCH}$ Karplus equations[13−15] were insufficient because the effect of substituent stereochemistry had not been considered.

DeMon-NMR Scaling. Also shown in Figure 3 is that the $^3J_{COCH}$ values calculated by deMon-NMR are generally too large when compared to those predicted by either the Serianni or the Tvaroska equations. Therefore, before beginning to develop a new Karplus equation, it was necessary to determine whether the deMon-NMR calculated $^3J_{COCH}$ values required scaling as was reported for other ab initio calculated coupling constants.[12,28]

TABLE 2: Coefficients for Eqs 1−3

	eq			
coefficient	2	1-α	1-β	3
A	8.14	8.14	8.14	8.14
B	−0.61	−0.61	−0.61	−0.61
C	−0.15	−0.15	−0.15	−0.15
D_α		0.71		
D_β			0.72	
D_{avg}				0.71
E_α		1.46		
E_β			1.47	
E_{avg}				1.46
F_α		44.3		
F_β			40.1	
F_{avg}				42
G		1.26	1.26	1.26
H		0.62	0.62	0.62
reduced χ^2	35.7	18.9	25.2	22.0

To assess this, several of the compounds (**9**−**12**, Figure 4) used to develop the previous experimental $^3J_{COCH}$ Karplus equations were optimized at the B3LYP/6-31G* level of theory. The $^3J_{COCH}$ values were then calculated with the deMon-NMR program and compared to the experimental values. Analysis of the results (Table 1) showed that the calculated deMon-NMR $^3J_{COCH}$ values are typically too large by an average of 16.7% and therefore should be scaled by 0.833. This scaling factor is consistent with those used in previous reports.[12,28]

Karplus Equation Development. The purpose of this study was to develop a single Karplus equation relating $^3J_{C1,H4}$ and the $C_1-O_4-C_4-H_4$ dihedral angle that would be applicable to all aldopentofuranosides. The observed influence (Figure 3) of anomeric stereochemistry on the magnitude of $^3J_{C1,H4}$ suggested that terms must be included that address this structural feature.

Drawing from previous work on the development of $^3J_{H,H}$ Karplus relationships,[8] the data were fit to an equationof the form of eq 1.

$$^3J_{C1,H4} = A\cos^2\theta + B\cos\theta + C + G[D - E\{\cos^2(\theta(\xi) + F \times G)]\} + H[D - E\{\cos^2(-\theta(\xi) + F \times H)]\} \quad (1)$$

In this equation, parameters $A-F$ can be optimized to best fit the data set, while parameters G and H are the electronegativities of the substituents at C_1. The ξ term is +1 for α-glycosides and −1 for β-glycosides. This form of the Karplus equation would therefore be general for all furanose rings and could be parametrized for any substituent at the anomeric center (e.g., a nucleoside base) by substitution of the appropriate group's electronegativity into the equation.

A three step process was used to develop the appropriate equation. First, the scaled $^3J_{C1,H4}$ values of all methyl furanosides **1**−**8** (240 data points) were fit to a truncated version of eq 1, which included only parameters $A-C$. This fitting procedure provided eq 2.

$$^3J_{C1,H4} = 8.14\cos^2\theta - 0.61\cos\theta - 0.15 \quad (2)$$

Second, using these values for $A-C$, the effect of stereochemistry at the anomeric center was taken into account by fitting the data for the α-glycosides in Figure 2 to the full eq 1.[29] The result was eq 1-α. The same procedure was used with the coupling constants from the β-glycosides to provide eq 1-β. The values for $D-F$ for these equations are given in Table 2, and the magnitudes of these parameters for both equations are very

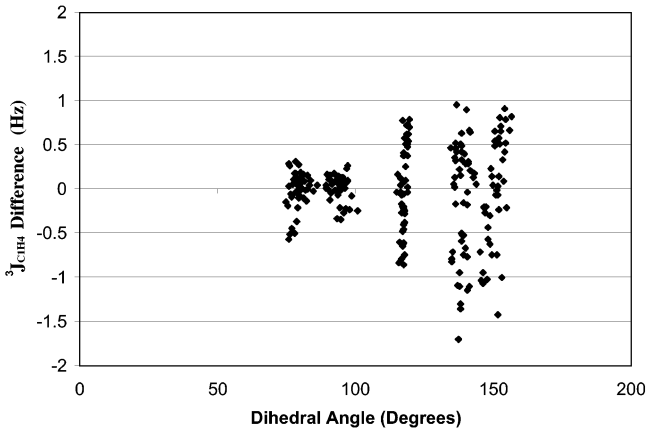

Figure 5. Plot of the difference between the $^3J_{C1,H4}$ calculated by Karplus eqs 1-α and 1-β and the $^3J_{C1,H4}$ calculated by deMon-NMR for **1**−**8** (Karplus equations−deMon-NMR).

similar. Finally, averaging of the $D-F$ values from eqs 1-α and 1-β yielded the general Karplus eq 3.

$$^3J_{C1,H4} = 8.14\cos^2\theta - 0.61\cos\theta - 0.15 + G[0.71 - 1.46\{\cos^2(\theta(\xi) + 44.3G)]\} + H[0.71 - 1.46\{\cos^2(-\theta(\xi) + 44.3H)]\} \quad (1\text{-}\alpha)$$

$$^3J_{C1,H4} = 8.14\cos^2\theta - 0.61\cos\theta - 0.15 + G[0.72 - 1.47\{\cos^2(\theta(\xi) + 40.1G)]\} + H[0.72 - 1.47\{\cos^2(-\theta(\xi) + 40.1H)]\} \quad (1\text{-}\beta)$$

$$^3J_{C1,H4} = 8.14\cos^2\theta - 0.61\cos\theta - 0.15 + G[0.71 - 1.46\{\cos^2(\theta(\xi) + 42G)]\} + H[0.71 - 1.46\{\cos^2(-\theta(\xi) + 42H)]\} \quad (3)$$

Calculating the reduced χ^2 value for eqs 1−3 allowed us to assess the goodness-of-fit of these equations to the data.[30] As shown in Table 2, any of the three forms of eq 1 are superior to eq 2 and averaging the values of $D-F$ from eqs 1-α and 1-β had only a minimal effect on the ability of this relationship to accurately reproduce the coupling constant data. To further check the fit of this equation to the data, the differences between the deMon-NMR calculated $^3J_{C1,H4}$ values and those predicted by eq 3 were calculated as a function of dihedral angle (Figure 5). The even distribution of error above and below zero reflects the quality of the fitting procedure. A comparison of the curve produced by eq 3 with that proposed[15] by Serianni shows much similarity (Figure 6). The α-glycoside curve lies just below, and the β-glycoside curve lies slightly above that derived from Serianni's equation (eq 4).[31]

$$^3J_{C1,H4} = 7.49\cos^2\theta - 0.96\cos\theta - 0.15 \quad (4)$$

A significant advantage of eq 3, however, is that it can be applied to any tetrahydrofuran ring-containing molecule through substitution of the appropriate group electronegativities.

Assessing the Conformational Preferences of Furanosides 1−8. With eq 3 in hand, it was possible to further clarify the conformational preferences of methyl glycosides **1**−**8**. PSEUROT analyses of the ring $^3J_{H,H}$ in **1**−**8** were done as described in the Methods section. When carrying out these analyses, it is necessary to provide the program with starting N and S conformers that are subsequently optimized. For each ring system, a series of four calculations, differing only in the identities of the starting N and S conformers, were done.[9a,11] The results of these calculations are presented in Table 3. Although for a given molecule some runs gave the same results, in all cases, more than one set of ring conformers can reproduce the experimentally measured $^3J_{H,H}$. With some ring systems (**6** and **7**), as many as three mathematically distinct solutions were found.

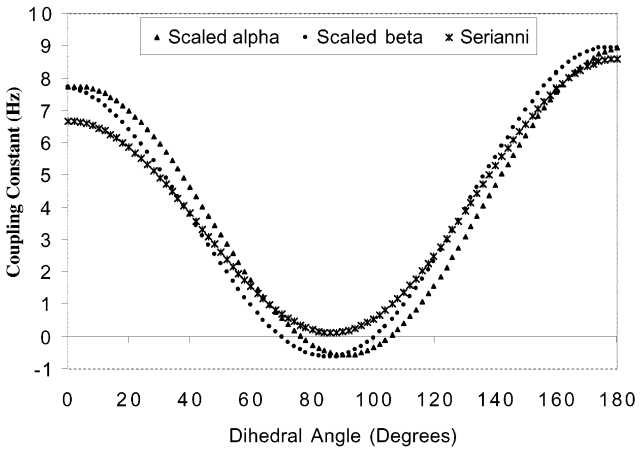

Figure 6. Comparison of Karplus curves generated from eqs 1-α (solid triangles), 1-β (solid circles), and 4 (×, ref 15).

TABLE 3: Results of PSEUROT Calculations for 1−8[a]

		compound							
run[b]		**1**	**2**	**3**	**4**	**5**	**6**	**7**	**8**
A	P_N	44	353	119	338	24	36	114	348
	%N	39	86	4	86	71	60	11	66
	P_S	123	162	125	85	145	139	122	265
	%S	61	14	96	14	29	40	89	34
	RMS[c]	0.0	0.0	0.1	0.0	0.0	0.0	0.1	0.0
B	P_N	70	353	37	28	20	36	309	27
	%N	67	86	29	73	65	60	39	45
	P_S	238	162	278	219	219	139	188	267
	%S	33	14	71	27	35	40	61	55
	RMS[c]	0.0	0.0	0.0	0.0	0.0	0.0	0.0	0.0
C	P_N	70	352	37	338	20	349	309	348
	%N	67	87	29	86	65	77	39	66
	P_S	238	187	278	85	219	305	188	265
	%S	33	13	71	14	35	23	61	34
	RMS[c]	0.0	0.1	0.0	0.0	0.0	0.3	0.0	0.0
D	P_N	70	353	37	338	24	345	324	348
	%N	67	86	29	86	71	74	8	66
	P_S	238	162	278	85	145	95	124	265
	%S	33	14	71	14	29	26	92	34
	RMS[c]	0.0	0.0	0.0	0.0	0.0	0.0	0.0	0.0

[a] See Supporting Information for coupling constants used. Calculated using a constant Φ_m (Altona−Sundaralingam puckering amplitude) = 39° for **1**−**8**. P = Altona−Sundaralingam pseudorotational phase angle. [b] Initial P_N and P_S values. Run A: $P_N = 50$, $P_S = 150$; run B: $P_N = 50$, $P_S = 250$; run C: $P_N = 320$, $P_S = 250$; run D: $P_N = 320$, $P_S = 150$. [c] In Hz.

For each conformer pair, we next calculated the expected magnitude of the experimental $^3J_{C1,H4}$ using the PSEUROT-derived conformer populations. This was done by the generation of graphs that correlated P in **1**−**8** with the $C_1-O_4-C_4-H_4$ dihedral angle (see Supporting Information). Armed with this information, it was possible to extract the dihedral angles for each ring conformer, which were then converted to the predicted $^3J_{C1,H4}$ for both members of the conformational ensemble using eq 3. The predicted $^3J_{C1,H4}$ values were then determined by taking a weighted average of these coupling constants based on the PSEUROT conformer populations.

Presented in Table 4 is a comparison of the $^3J_{C1,H4}$ calculated as described above (predicted $^3J_{C1,H4}$) with the value measured by experiment (exp $^3J_{C1,H4}$). For five of the eight compounds,

TABLE 4: Comparison of Experimental and Predicted $^3J_{C1,H4}$ in 1−8[a]

compd	predicted $^3J_{C1,H4}$[b] run A[c]	run B[c]	run C[c]	run D[c]	exp $^3J_{C1,H4}$
1 (α-arabino)	0.1	2.2	2.2	2.2	<0.5
2 (β-arabino)	1.3	1.3	1.6	1.3	3.2
3 (α-ribo)	0.1	3.6	3.6	3.6	<0.5
4 (β-ribo)	2.2	1.9	2.2	2.2	2.7
5 (α-lyxo)	0.3	2.0	2.0	0.3	3.7
6 (β-lyxo)	0.4	0.4	2.4	1.5	2.2
7 (α-xylo)	0.2	4.3	4.3	0.3	<0.5
8 (β-xylo)	3.1	3.7	3.1	3.1	2.4

[a] Coupling constants are in Hz. Structures are in Figure 2. [b] See text for the method by which these coupling constants were calculated. [c] See legend for Table 1 and the Methods section for definitions.

this coupling constant can be used to eliminate all but one of the solutions obtained from the PSEUROT calculations. For example, in the case of **1**, the value of $^3J_{C1,H4}$ measured from the ^{13}C NMR spectrum is <0.5 Hz, which correlates only with the mathematical solution obtained from run A. The other possible solution, obtained from runs B−D, predicted a magnitude of 2.2 Hz for $^3J_{C1,H4}$. Similar arguments can be used to select a single PSEUROT solution for **3** (run A), **5** (run B/C), **6** (run C), and **8** (run A/C/D).

In contrast, for methyl α-D-xylofuranoside, **7**, it was possible to eliminate only one of the three solutions. The experimental $^3J_{C1,H4}$ measured from the NMR spectrum is consistent with the conformers calculated from either run A or run D. We note, however, that the equilibrium predicted from these runs is heavily biased toward the same S conformer (run A: $P_S = 122°$, 89%; run D: $P_S = 124°$, 92%) and that the difference between these solutions is in the identity of the N conformer, which makes only a very small contribution to the overall conformational ensemble. Therefore, although the $^3J_{C1,H4}$ value did not allow us to unambiguously determine the conformation of the minor conformer in this equilibrium, it did allow us to rule out the solution that predicted a 60:40 N:S mixture of conformers with $P_N = 309°$ and $P_S = 188°$ (runs B/C).

For the remaining two molecules, methyl β-D-arabinofuranoside, **2**, and methyl β-D-ribofuranoside, **4**, the $^3J_{C1,H4}$ magnitude is uninformative as both PSEUROT solutions for these molecules would be expected to give a $^3J_{C1,H4}$ value of similar size. As with **7**, the predicted conformational ensemble of **2** and **4** is an equilibrium heavily biased to one conformer. In the case of **2**, all four runs gave the same predominant N conformer ($P_N = 352-353°$), which is similar to the conformation of the ring in the available crystal structure.[26a] Run C differs from the others in the identity of the minor S conformer (run C: $P_S = 187°$; runs A, B, and D: $P_S = 162°$). Although PSEUROT analysis of $^3J_{H,H}$ measured on **4** predicts an equilibrium biased toward the north, the two solutions differ in the identity of the major and minor conformers (run B: $P_N = 28°$; $P_S = 219°$; runs A, C, and D: $P_N = 338°$; $P_S = 85°$) and the $^3J_{C1,H4}$ cannot be used to differentiate between them.

In cases such as **2**, **4**, and **7**, other $^1H-^{13}C$ coupling constants could possibly be used to differentiate between the PSEUROT solutions. Measurement of these *J* values may, however, prove difficult using unlabeled substrates due to overlap in the proton-coupled ^{13}C NMR spectra. Furthermore, for rings such as **2** and **7**, in which the only difference between the two solutions is the identity of a minor conformer, it is unlikely that any parameter could unequivocally identify the structure of the minor species. For systems of this type, it may prove more feasible to probe the structure of the minor conformer by high-level computational methods.

TABLE 5: Results of PSEUROT Calculations for 1−8 Using $^3J_{H,H}$ Measured over a Range of Temperatures[a]

run[b]		compound **1**	**2**	**3**	**4**	**5**	**6**	**7**	**8**
A	Φ_m(N)	22	57	6	47	34	35	13	31
	P_N	60	47	16	358	37	38	26	348
	%N	82	70	71	57	85	66	36	78
	Φ_m(S)	33	38	56	4	32	42	45	42
	P_S	170	132	130	36	110	148	140	244
	%S	18	30	29	43	15	34	64	22
	RMS[c]	0.1	0.9	0.3	0.1	0.8	0.0	0.1	0.1
B	Φ_m(N)	26	57	7	57	47	38	12	31
	P_N	62	42	345	43	22	62	47	348
	%N	75	73	69	65	47	59	42	78
	Φ_m(S)	53	14	54	15	45	43	48	42
	P_S	226	199	305	234	235	190	142	244
	%S	25	27	31	35	53	41	58	22
	RMS[c]	0.1	0.8	0.1	0.1	0.0	0.0	0.1	0.1
C	Φ_m(N)	37	39	25	40	29	47	50	34
	P_N	328	341	321	323	312	318	284	345
	%N	74	88	65	84	52	47	41	79
	Φ_m(S)	17	29	23	29	57	57	42	41
	P_S	219	93	279	220	225	245	199	245
	%S	26	12	35	16	48	53	59	21
	RMS[c]	2.7	0.0	0.1	1.3	0.7	0.6	0.1	0.1
D	Φ_m(N)	57	39	24	40	39	46	12	34
	P_N	71	336	309	336	22	352	33	346
	%N	40	85	93	98	70	53	42	78
	Φ_m(S)	2	42	48	21	40	20	48	39
	P_S	268	157	120	180	141	98	145	246
	%S	60	15	7	2	30	47	58	22
	RMS[c]	0.1	0.8	0.1	0.3	0.0	0.0	0.1	0.1

[a] See Supporting Information for coupling constants used. P = Altona-Sundaralingam pseudorotational phase angle, Φ_m = Altona-Sundaralingam puckering amplitude. [b] Initial P_N and P_S values: Run A: $P_N = 50$, $P_S = 150$; Run B: $P_N = 50$, $P_S = 250$; Run C: $P_N = 320$, $P_S = 250$; Run D: $P_N = 320$, $P_S = 150$. [c] In Hz.

In general, the predicted $^3J_{C1,H4}$ values agreed well with those measured by experiment; however, in some cases (e.g., **2**, **5**, and **8**), the agreement was poorer. As described above, the predicted $^3J_{C1,H4}$ values were obtained from the PSEUROT results and any inaccuracies in these analyses will be reflected in the expected magnitude of this coupling constant. Although the RMS errors in these PSEUROT calculations are excellent (see Table 3), it should be appreciated that in these rings only three $^3J_{H,H}$ values are available for analysis ($^3J_{H1,H2}$, $^3J_{H2,H3}$, and $^3J_{H3,H4}$). Five parameters are required to describe the conformation of these rings (the P and Φ_m of both conformers and the percentage of one of them); therefore, the system is underdetermined. The results presented in Table 3 were calculated by using an approach that is standard[9a,b,11] in these analyses: the Φ_m of both conformers is kept fixed (39° in this study). However, the validity of setting the Φ_m of both conformers to a fixed value can be questioned and to obtain additional data for these PSEUROT calculations, we have measured NMR spectra for **1**−**8** over a range of temperatures (35, 45, 55, 65, 75, and 85 °C). Using the coupling constants measured from all of the spectra recorded over this temperature range, it was possible to perform the PSEUROT analyses in which all five parameters were allowed to optimize. The coupling constants measured from these variable temperature NMR experiments are provided in the Supporting Information; the results of the subsequent PSEUROT calculations are given in Table 5.

TABLE 6: Comparison of Experimental and Predicted $^3J_{C1,H4}$ in 2, 5, and 8 Using PSEUROT Conformer Populations Obtained from $^3J_{H,H}$ Values Measured over a Range of Temperatures[a]

	predicted $^3J_{C1,H4}$[b]				
compd	run A[c]	run B[c]	run C[c]	run D[c]	exp $^3J_{C1,H4}$
2 (β-arabino)	*d*	*d*	2.1	2.8	3.2
5 (α-lyxo)	0.0	3.4	*d*	0.4	3.7
6 (β-lyxo)	0.6	2.1	*d*	*d*	2.2
8 (β-xylo)	2.8	2.8	2.9	2.9	2.4

[a] Coupling constants are in Hz. [b] See text for the method by which these coupling constants were calculated. [c] See legend for Table 1 and the Methods section for definitions. [d] Not calculated.

Comparison of the data in Tables 3 and 5 shows that in some cases, the results are similar. However, when the Φ_m was not kept fixed, one or both conformers often optimized to puckering amplitudes that were either unreasonably high (57°) or low (2°). For compounds **2**, **5**, **6**, and **8**, the conformer identities and populations presented in Table 5 were used to calculate predicted $^3J_{C1,H4}$ values. In these calculations, we used only those PSEUROT solutions in which the Φ_m of both conformers was between 29 and 49° as we considered structures with larger or smaller puckering amplitudes as physically unlikely. For the same reason, we have not performed these calculations for any of the conformer pairs given in Table 5 for **1**, **3**, **4**, and **7**. The predicted $^3J_{C1,H4}$ values for **2**, **5**, **6**, and **8** are shown in Table 6 and are compared to the experimental magnitude of this coupling constant. For all four compounds, one of the predicted $^3J_{C1,H4}$ values agrees closely with the experimental coupling constant. For **2**, **5**, and **8**, the agreement between the predicted and the experimental $^3J_{C1,H4}$ values is significantly better than those calculated using the PSEUROT results with a fixed Φ_m (Table 4).

These investigations have allowed us to further clarify the conformational preferences of methyl glycosides **1**−**8**. The PSEUROT solutions that best fit the measured $^3J_{H,H}$ and $^3J_{C1,H4}$ data using both the fixed puckering (FP) amplitude and optimized puckering (OP) amplitude approaches are listed in Table 7. This information was compiled from the data in Tables 3−6 and is compared to available crystal structure data.[26] Although it was not always possible to identify a single conformer pair that best fits the measured coupling constant data, the combined use of $^3J_{H,H}$ and $^3J_{C1,H4}$ has allowed us to narrow the number of conformer solutions using a method other than intuition. With some of these compounds (e.g., **1**), the FP approach leads to results that are consistent with the experimental $^3J_{C1,H4}$ magnitude. In other cases (e.g., **2**), better agreement between the predicted and the experimental $^3J_{C1,H4}$ value is obtained by the OP approach, in which these analyses are carried out with a larger number of measured $^3J_{H,H}$ and the puckering amplitudes (Φ_m) are not fixed. However, we have found that the OP approach often leads to solutions in which one or both of the conformers have puckering amplitudes significantly larger or smaller than is likely.

When comparing the PSEUROT results for a given molecule using the FP vs OP approach, the agreement between the two methods varies. For **2**, **6**, and **8**, similar results are obtained, while for the compounds with the *β-lyxo* stereochemistry (**5**), the agreement is poorer. This comparison was not possible for **1**, **3**, **4**, and **7** because the OP amplitude approach only gave solutions with physically unreasonable Φ_m values. Finally, the data presented in Table 7 are consistent with available crystal structures[26] for **1**, **2**, **4**, **5**, and **7**, in that the ring conformation in the crystal structure is similar to one (usually the major) solution conformer. The average Φ_m in these crystal structures is 38° with a range of 35−45°, which is also consistent with the puckering amplitudes provided in Table 7.

Conclusions

This report has detailed the development of a Karplus equation that accounts for the effects of anomeric stereochemistry upon the magnitude of the $^3J_{C1,H4}$ in aldopentofuranosides. Derivation of this equation was achieved first by calculating (deMon-NMR) the $^3J_{C1,H4}$ values for 30 B3LYP/6-31G* optimized envelope geometries of each methyl aldopentofuranoside (Figure 2) to provide a data set of 240 coupling constants. These data were then fit to a six term Karplus equation to give eq 3, which is applicable to all aldopentofuranosides. After its development, eq 3 was used to further clarify the ring conformational preferences of methyl furanosides **1**−**8**. Although there are limitations in the use of this approach, it can be used as a method to clarify the results of PSEUROT calculations derived only from $^3J_{H,H}$ magnitudes.

It should be possible to apply eq 3 to tetrahydrofuran rings that contain other substituents at the anomeric center through the substitution of the appropriate group electronegativity into the equation; however, some reparametrization may be necessary. Efforts toward the application of this equation to other tetrahydrofuran rings is currently in progress both experimentally and computationally.

TABLE 7: Preferred Conformations of 1−8 as Determined by a Combination of PSEUROT and $^3J_{C1,H4}$ Analysis[a]

	with Φ_m[b] fixed at 39°				with optimized Φ_m[b]						crystal[f]	
compd	P_N[c]	% N	P_S[c]	% S	P_N[c]	% N	P_S[c]	% S	Φ_m(N)[b]	Φ_m(S)[b]	P[c]	Φ_m[b,h]
1 (α-arabino)	44	39	123	61	*d*	*d*	*d*	*d*	*d*	*d*	54	39
	e	*e*	*e*	*e*	*e*	*e*	*e*	*e*	*e*	*e*	58	38
2 (β-arabino)	353	87	162	13	336	85	157	15	39	42	326	39
	352	86	187	14	341	88	93	12	39	39	*g*	*g*
3 (α-ribo)	119	4	125	96	*d*	*d*	*d*	*d*	*d*	*d*	*g*	*g*
4 (β-ribo)	338	86	85	14	*d*	*d*	*d*	*d*	*d*	*d*	337	35
	28	73	219	27	*d*	*d*	*d*	*d*	*d*	*d*	349	43
5 (α-lyxo)	20	65	219	35	22	47	235	53	47	45	27	43
6 (β-lyxo)	349	77	305	23	62	59	190	41	38	43	*g*	*g*
7 (α-xylo)	324	8	124	92	*d*	*d*	*d*	*d*	*d*	*d*	160	40
8 (β-xylo)	348	66	265	34	348	78	244	22	31	42	*g*	*g*
	e	*e*	*e*	*e*	345	79	245	21	34	41	*g*	*g*
	e	*e*	*e*	*e*	346	78	246	22	34	39	*g*	*g*

[a] Compiled from Tables 3−6 and ref 26. [b] Φ_m = Altona−Sundaralingam puckering amplitude. [c] P = Altona−Sundaralingam pseudorotational phase angle. [d] In all mathematical solutions, one or both conformers had a Φ_m magnitude outside the 29−49° range. [e] Not applicable. [f] Compounds **1** and **4** have two molecules in the asymmetric unit cell. [g] No crystal structure is available. [h] Φ_m were calculated by multiplying the Cremer-Pople puckering amplitudes in ref 26 by 100.

Acknowledgment. This work was funded by grants from the National Science Foundation (CHE-9875163 and CHE-9733457) and the Ohio Supercomputer Center. J.B.H. is supported as a graduate research fellow by a NIH Training Grant for Chemistry at the Biology Interface. We also thank Frank deLucia, Kristin Huchton, and Dr. Terry Gustafson for assistance with the statistical analysis.

Supporting Information Available: Experimental $^3J_{H,H}$, deMon-NMR calculated $^1J_{C1,H4}$, and graphs of P vs $C_1-O_4-C_4-H_4$ dihedral angles for **1**−**8**. This material is available free of charge via the Internet at http://www.acs.org.

References and Notes

(1) Saenger, W. *Principles of Nucleic Acid Structure*; Spring-Verlag: Berlin, 1988.

(2) (a) Brennan, P. J.; Nikaido, H. *Annu. Rev. Biochem.* **1995**, *64*, 29. (b) Gerold, P.; Eckert, V.; Schwarz, R. T. *Trends Glycosci. Glycotechnol.* **1996**, *8*, 265. (c) de Lederkremer, R. M.; Colli, W. *Glycobiology* **1995**, *5*, 547. (d) Unkefer, C. J.; Gander, J. *J. Biol. Chem.* **1990**, *265*, 685. (e) Mendonça-Previato, L.; Gorin, P. A. J. *Infect. Immun.* **1980**, *29*, 934. (f) Groisman, J. F.; de Lederkremer, R. M. *Eur. J. Biochem.* **1987**, *165*, 327.

(3) (a) Ryder, M. H.; Tate, M. E.; Jones, G. P. *J. Biol. Chem.* **1984**, *259*, 9704. (b) Komatsu, K.; Shigemori, H.; Kobayashi, J. *J. Org. Chem.* **2001**, *66*, 6189.

(4) Altona, C.; Sundaralingam, M. *J. Am. Chem. Soc.* **1972**, *94*, 8205.

(5) Altona, C.; Sundaralingam, M. *J. Am. Chem. Soc.* **1973**, *95*, 2333.

(6) (a) Kilpatrick, J. E.; Pitzer, K. S.; Spitzer, R. *J. Am. Chem. Soc.* **1947**, *69*, 2483. (b) Pitzer, K. S.; Donath, W. F. *J. Am. Chem. Soc.* **1959**, *81*, 3213.

(7) (a) Haasnoot, C. A. G.; de Leeuw, F. A. A. M.; Altona, C. *Tetrahedron* **1980**, *36*, 2783. (b) Haasnoot, C. A. G.; de Leeuw, F. A. A. M.; de Leeuw, H. P. M.; Altona, C. *Org. Magn. Reson.* **1981**, *15*, 43.

(8) (a) Altona, C.; Francke, R.; de Haan, R.; Ippel, J. H.; Daalmans, G. J.; Westra Hoekzema, A. J. A.; van Wijk, J. *Magn. Reson. Chem.* **1994**, *32*, 670. (b) van Wijk, J.; Huckriede, B. D.; Ippel, J. H.; Altona, C. *Methods Enzymol.* **1992**, *211*, 286.

(9) (a) van Wijk, J.; Haasnoot, C. A. G.; de Leeuw, F. A. A. M.; Huckriede, B. D.; Westra Hoekzema, A.; Altona, C. *PSEUROT 6.2*; Leiden Institute of Chemistry, Leiden University: Leiden, 1993; *PSEUROT 6.3*; Leiden Institute of Chemistry, Leiden University: Leiden, 1999. (b) de Leeuw, F. A. A. M.; Altona, C. *J. Comput. Chem.* **1983**, *4*, 428. (c) Altona, C. *Recl. Trav. Chem. Pays-Bas* **1982**, *101*, 413.

(10) Selected examples: (a) de Leeuw, F. A. A. M.; Altona, C.; Kessler, H.; Bermal, W.; Friedrich, A.; Krack, G.; Hull. W. *J. Am. Chem. Soc.* **1983**, *105*, 2237. (b) Haasnoot, C. A. G.; de Leeuw, F. A. A. M.; de Leeuw, H. P. M.; Altona, C. *Biopolymers* **1981**, *20*, 1211. (c) Crnugelj, M.; Dukhan, D.; Barascut, J.-L.; Imbach, J.-L.; Plavec, J. *J. Chem. Soc., Perkin Trans. 2* **2000**, 255. (d) Thibaudeau, C.; Kumar, A.; Bekiroglu, S.; Matsuda, A.; Marquez, V. E. Chattopadhyaya, J. *J. Org. Chem.* **1998**, *63*, 5447. (e) Callam, C. S.; Lowary, T. L. *J. Org. Chem.* **2001**, *67*, 8961. (f) Thibaudeau, C.; Kumar, A.; Bekiroglu, S.; Matsuda, A.; Marquez, V. E. Chattopadhyaya, J. *J. Org. Chem.* **1998**, *63*, 5447. (g) Barchi, J. J., Jr.; Jeong, L. S.; Siddiqui, M. A.; Marquez, V. E. *J. Biochem. Biophys. Methods* **1997**, *34*, 11. (h) Acharya, P.; Nawrot, B.; Sprinzl, M.; Thibaudeau, C.; Chattopadhyaya, J. *J. Chem. Soc., Perkin Trans. 2* **1999**, 1531.

(11) Hoffman, R. A.; van Wijk, J.; Leeflang, B. R.; Kamerling, J. P.; Altona, C.; Vliegenthart, J. F. G. *J. Am. Chem. Soc.* **1992**, *114*, 3710.

(12) (a) Church, T. J.; Carmichael, I.; Serianni, A. S. *J. Am. Chem. Soc.* **1997**, *119*, 8946. (b) Podlasek, C. A.; Stripe, W. A.; Carmichael, I.; Shang, M.; Basu, B. Serianni, A. S. *J. Am. Chem. Soc.* **1996**, *118*, 1413.

(13) Mulloy, B.; Frenkiel, T. A.; Davies, D. B. *Carbohydr. Res.* **1988**, *184*, 39.

(14) Tvaroska, I.; Hricovini, H.; Petrakova, E. *Carbohydr. Res.* **1989**, *189*, 359.

(15) Cloran, F.; Carmichael, I.; Serianni, A. S. *J. Am. Chem. Soc.* **1999**, *121*, 9843.

(16) (a) Gordon, M. T.; Lowary, T. L.; Hadad, C. M. *J. Am. Chem. Soc.* **1999**, *121*, 9682. (b) D'Souza, F. W.; Ayers, J. D.; McCarren, P. R.; Lowary, T. L. *J. Am. Chem. Soc.* **2000**, *122*, 1251. (c) Gordon, M. T.; Lowary, T. L.; Hadad, C. M. *J. Org. Chem.* **2000**, *65*, 4954. (d) McCarren, P. R.; Gordon, M. T.; Lowary, T. L.; Hadad, C. M. *J. Phys. Chem. A* **2001**, *105*, 5911. (e) Callam, C. S.; Singer, S. J.; Lowary, T. L.; Hadad, C. M. *J. Am. Chem. Soc.* **2001**, *123*, 11743.

(17) (a) Labanowski, J. W.; Andzelm, J. *Density Functional Methods in Chemistry*; Springer: New York, 1991. (b) Parr, R. G.; Yang, W. *Density Functional Theory in Atoms and Molecules*; Oxford University Press: New York, 1989.

(18) Frisch, M. J.; Trucks, G. W.; Schlegel, H. B.; Scuseria, G. E.; Robb, M. A.; Cheeseman, J. R.; Zakrzewski, V. G.; Montgomery, J. A., Jr.; Stratmann, R. E.; Burant, J. C.; Dapprich, S.; Millam, J. M.; Daniels, A. D.; Kudin, K. N.; Strain, M. C.; Farkas, O.; Tomasi, J.; Barone, V.; Cossi, M.; Cammi, R.; Mennucci, B.; Pomelli, C.; Adamo, C.; Clifford, S.; Ochterski, J.; Petersson, G. A.; Ayala, P. Y.; Cui, Q.; Morokuma, K.; Malick, D. K.; Rabuck, A. D.; Raghavachari, K.; Foresman, J. B.; Cioslowski, J.; Ortiz, J. V.; Stefanov, B. B.; Liu, G.; Liashenko, A.; Piskorz, P.; Komaromi, I.; Gomperts, R.; Martin, R. L.; Fox, D. J.; Keith, T.; Al-Laham, M. A.; Peng, C. Y.; Nanayakkara, A.; Gonzalez, C.; Challacombe, M.; Gill, P. M. W.; Johnson, B. G.; Chen, W.; Wong, M. W.; Andres, J. L.; Head-Gordon, M.; Replogle, E. S.; Pople, J. A. *Gaussian 98*, revision A.9; Gaussian, Inc.: Pittsburgh, PA, 1998.

(19) The gas-phase geometries do not differ significantly from those obtained by optimization using a solvation model (ref 20).

(20) Houseknecht, J. B.; Altona, C.; Hadad, C. M.; Lowary, T. L. *J. Org. Chem*. **2002**, *67*, 4647.

(21) (a) Becke, A. D. *Phys. Rev. A* **1988**, *38*, 3098. (b) Becke, A. D. *J. Chem. Phys.* **1993**, *98*, 5648. (c) Lee, C.; Yang, W.; Parr, R. G. *Phys. Rev. B* **1988**, *37*, 785. (d) Hehre, W. J.; Radom, L.; Schleyer, P. v. R.; Pople, J. A. *Ab Initio Molecular Orbital Theory*; John Wiley & Sons: New York, 1986.

(22) (a) St-Amant, A.; Salahub, D. R. *Chem. Phys. Lett.* **1990**, *169*, 387. (b) Casida, M. E.; Daul, C.; Goursot, A.; Koester, A.; Pettersson, L.; Proynov, E.; St-Amant, A.; Salahub, D. R.; Duarte, H.; Godbout, N.; Guan, J.; Jamorski, C.; Leboeuf, M.; Malkin, V.; Malkina, O.; Sim, F.; Vela, A. *deMon-KS*, version 3.4; deMon Software: 1996. (c) Malkin, V. G.; Malkina, O. L.; Salahub, D. R. *Chem. Phys. Lett.* **1994**, *221*, 91. (d) Malkina, O. L.; Salahub, D. R.; Malkin, V. G. *J. Chem. Phys.* **1996**, *105*, 8793. (e) Salahub, D. R.; Fournier, R.; Mlynarski, P.; Papai, I.; St-Amant, A.; Uskio, J. In *Density Functional Methods in Chemistry*; Labanowski, J. K., Anzelm, J. W., Eds.; Springer: New York, 1991; p 77. (f) Malkin, V. G.; Malkina, O. L.; Casida, M. E.; Salahub, D. R. *J. Am. Chem. Soc.* **1994**, *116*, 5898.

(23) (a) Perdew, J. P.; Wang, Y. *Phys. Rev. B* **1986**, *33*, 8800. (b) Perdew, J. P. *Phys. Rev. B* **1986**, *33*, 8822. (c) Perdew, J. P. *Phys. Rev. B* **1986**, *34*, 7406.

(24) Fletcher, H. G. *Methods Carbohydr. Chem.* **1963**, *2*, 228.

(25) Serianni, A. S.; Barker, R. *J. Org. Chem.* **1984**, *49*, 3292.

(26) (a) Evdokimov, A.; Gilboa, A. J.; Koetzle, T. F.; Klooster, W. T.; Schultz, A. J.; Mason, S. A.; Albinati, A.; Frolow, F. *Acta Crystallogr. B* **2001**, *57*, 213. (b) Evdokimov, A. G.; Kalb, A. J.; Koetzle, T. F.; Klooster, W. T.; Martin, J. M. L. *J. Phys. Chem. A* **1999**, *103*, 744. (c) Podlasek, C. A.; Stripe, W. A.; Carmichael, O.; Shang, M.; Basu, B.; Serianni, A. S. *J. Am. Chem. Soc.* **1996**, *118*, 1413.

(27) Fixing the puckering amplitude to 34° yielded PSUEROT populations that were not significantly different from those obtained when this value was fixed at 39°.

(28) Houseknecht, J. B.; McCarren, P. R.; Lowary, T. L.; Hadad, C. M. *J. Am. Chem. Soc.* **2001**, *123*, 8811.

(29) This was done using the Marquardt−Levenberg method as implemented in SigmaPlot for Windows 6.0, SPSS, Inc.

(30) The χ^2 values were determined by squaring the difference between the deMon calculated $^3J_{C1,H4}$ and that calculated by the Karplus equation and then dividing that value by 0.01 (a standard deviation of 0.1 Hz was assumed) multiplied by the number of data points.

(31) The $^3J_{C1,H4}$ calculated by deMon-NMR for $C_1-O_4-C_4-H_4$ dihedral angles between 80 and 100° were negative. Consequently, the coupling constants predicted within this dihedral angle range by eqs 1-α, 1-β, and 3 are also negative. We chose not to add a scaling factor to our coupling constants to address the negative J values.